World Journal of Gastroenterology

Submit a Manuscript: http://www.wjgnet.com/esps/

World J Gastroenterol 2017 March 7; 23(9): 1666-1675

DOI: 10.3748/wjg.v23.i9.1666

ISSN 1007-9327 (print) ISSN 2219-2840 (online)

ORIGINAL ARTICLE

Prospective Study

Spectral computed tomography in advanced gastric cancer: Can iodine concentration non-invasively assess angiogenesis?

Xiao-Hua Chen, Ke Ren, Pan Liang, Ya-Ru Chai, Kui-Sheng Chen, Jian-Bo Gao

Xiao-Hua Chen, Pan Liang, Ya-Ru Chai, Jian-Bo Gao, Department of Radiology, The First Affiliated Hospital of Zhengzhou University, Zhengzhou 450052, Henan Province, China

Ke Ren, Surgery of Gastroenterology, Luohe Central Hospital, Luohe 462000, Henan Province, China

Kui-Sheng Chen, Department of Pathology, The First Affiliated Hospital of Zhengzhou University, Zhengzhou 450052, Henan Province, China

Author contributions: Chen XH and Ren K performed the research, data analysis and wrote the paper; Liang P contributed to the statistical analysis; Chai YR collected the data and assigned the forms; Chen KS performed the pathological examinations; Gao JB designed the research and contributed to the paper revisions.

Supported by the National Natural Science Foundation of China, No.81271573.

Institutional review board statement: The study was reviewed and approved by the institutional review boards of the First Affiliated Hospital of Zhengzhou University.

Informed consent statement: All study participants provided informed written consent prior to study enrollment.

Conflict-of-interest statement: The authors declare no conflicts of interest.

Data sharing statement: No additional data are available.

Manuscript source: Unsolicited manuscript

Correspondence to: Jian-Bo Gao, Professor, Department of Radiology, The First Affiliated Hospital of Zhengzhou University, No. 1, East Jianshe Road, Zhengzhou 450052, Henan Province, China. jianbogaochina@163.com
Telephone: +86-371-67966890
Fax: +86-371-66970906

Received: November 24, 2016
Peer-review started: November 26, 2016
First decision: January 10, 2017
Revised: January 19, 2017
Accepted: February 7, 2017
Article in press: February 8, 2017
Published online: March 7, 2017

Abstract

AIM

To investigate the correlation of iodine concentration (IC) generated by spectral computed tomography (CT) with micro-vessel density (MVD) and vascular endothelial growth factor (VEGF) expression in patients with advanced gastric carcinoma (GC).

METHODS

Thirty-four advanced GC patients underwent abdominal enhanced CT in the gemstone spectral imaging mode. The IC of the primary lesion in the arterial phase (AP) and venous phase (VP) were measured, and were then normalized against that in the aorta to provide the normalized IC (nIC). MVD and VEGF were detected by immunohistochemical assays, using CD34 and VEGF-A antibodies, respectively. Correlations of nIC with MVD, VEGF, and clinical-pathological features were analyzed.

RESULTS

Both nICs correlated linearly with MVD and were higher in the primary lesion site than in the normal control site, but were not correlated with VEGF expression. After stratification by clinical-pathological subtypes, nIC-AP showed a statistically significant correlation with MVD, particularly in the group with tumors at stage T4, without nodular involvement, of a mixed Lauren type, where the tumor was located at the antrum site, and occurred in female individuals. nIC-VP showed a positive correlation with MVD in the group with the tumor at stage T4 and above, had nodular involvement, was poorly differentiated, was located at the pylorus site, of a mixed and diffused Lauren subtype, and occurred in male individuals. nIC-AP and nIC-VP showed significant differences in terms of histological differentiation and Lauren subtype.

CONCLUSION

The IC detected by spectral CT correlated with the MVD. nIC-AP and nIC-VP can reflect angiogenesis in different pathological subgroups of advanced GC.

Key words: Micro-vessel density; Iodine concentration; Spectral computed tomography; Vascular endothelial growth factor; Gastric cancer

Core tip: We investigated the correlation between iodine concentration (IC) value generated from spectral computed tomography (CT) and angiogenesis in gastric cancer (GC) with clinical-pathological data. Our results showed that normalized IC (nIC) in both the arterial (AP) and venous phases (VP) had a positive linear correlation with micro-vessel density. nIC-AP reflected the angiogenesis in relatively earlier and well-differentiated GC, while nIC-VP reflected this in further advanced and poorly differentiated GC. Spectral CT with quantitative IC value offers a new choice for evaluating the angiogenesis of gastric cancer noninvasively.

Chen XH, Ren K, Liang P, Chai YR, Chen KS, Gao JB. Spectral computed tomography in advanced gastric cancer: Can iodine concentration non-invasively assess angiogenesis? *World J Gastroenterol* 2017; 23(9): 1666-1675 Available from: URL: http://www.wjgnet.com/1007-9327/full/v23/i9/1666.htm DOI: http://dx.doi.org/10.3748/wjg.v23.i9.1666

INTRODUCTION

Despite a recent decrease, gastric cancer (GC) remains the most common cancer and is the third leading cause of cancer-related death globally[1]. In China, the incidence and mortality rates of GC remain high, and the vast majority of cases are in the advanced stage[2], which requires more attention.

Angiogenesis is fundamental to the growth, invasion, and metastasis of GC, and greatly influences the response to anti-tumor therapies[3]. To date, the standard method for studying angiogenesis has been histopathological counting of micro-vessel density (MVD), which is specimen- and immunostaining-dependent. This is impractical in advanced patients undergoing anti-angiogenesis or chemotherapy. Compared with MVD counting, using preoperative imaging modalities for the noninvasive assessment of tumor angiogenesis is more acceptable and feasible. A previous study has revealed that MVD, vascular endothelial growth factor (VEGF), and the absolute enhanced value show some positive correlations with conventional contrast-enhanced computed tomography (CT)[4]. Additionally, CT perfusion has shown the potential for evaluating tumor angiogenesis[5,6], but the complicated measurement and high radiation dosage have limited the extensive application of CT in this regard.

The recently developed spectral CT yields material-decomposition (MD) images that can quantitatively map the iodine concentration (IC) of the tissue in enhanced images. This IC value has been proven to show a strong correlation with the actual iodine concentration in the phantom[7]. Recently, preliminary studies have reported the use of the IC value to differentiate benign and malignant lesions, to find embolisms, and to evaluate the efficacy of anticancer therapy[8-11]. Particularly in the evaluation of neoadjuvant chemotherapy of GC, the IC value was proven to be a more robust imaging biomarker than the morphology index[11]. However, it was not clear how this correlated with radiological-pathological features. On the other hand, the IC value has shown a correlation with vascularization in solid tumors, such as pancreatic carcinoma, hepatocarcinoma, and non-small-cell lung cancer[12-14], while there has been no such report for GC, to provide a basis for using image indicators, other than morphology, for assessing chemo-efficacy. Therefore, our purpose was to investigate the correlation between IC value and angiogenesis in GC cases with clinical-pathological data.

MATERIALS AND METHODS

Study population

Adult patients with advanced GC confirmed by endoscopic biopsy, who were scheduled for surgery, were enrolled. This study was approved by the institutional review board, and informed consent was obtained from each participant. All procedures were performed in accordance with the ethical standards of the institution.

Exclusion criteria were: (1) allergies to intravenous contrast media; (2) cardiac or renal insufficiency; (3) history of chemotherapy or radiotherapy; (4) inability to visualize the tumor on CT; (5) early tumor staging (T1) or presence of distant metastasis (M1); and (6)

specimen with poor fixation for immunostaining.

From June 2014 to May 2015, a total of 41 patients prospectively underwent spectral CT examination. Of these, two patients with serious interface artifacts on CT images, one patient with tumor tissue necrosis that influenced MVD counting, one patient with no tumor cells on hematoxylin and eosin (HE) slices, and three patients with failed immunostaining were excluded.

Ultimately, the data of 34 patients were collected and statistically analyzed. Patient records and pathological data, including gender, age, tumor size, tumor location, invasion depth, lymph nodes involvement, Lauren subtypes, and differentiation, were documented.

CT scan methods

After fasting overnight, all patients were administered 10 mg anisodamine (Minsheng Pharmaceutical Group Co., Ltd., Hangzhou, China) intramuscularly to reduce gastrointestinal motility 20 min prior to CT examination, and ingested 800-1000 mL of water to distend the stomach. During scanning, patients were instructed to suspend respiration.

All examinations were performed on a Discovery CT750 HD system (GE Healthcare, Milwaukee, WI, United States), and included bi-phasic enhanced spectral scanning in the arterial and venous phases (AP and VP, respectively). Spectral CT imaging was performed with a 0.5 ms switch of tube voltage between 140 kVp and 80 kVp; a rotation speed of 0.6 s, and a helical pitch of 1.375:1. The scan range was from the diaphragmatic dome to the symphysis pubis. Non-ionic contrast material, iohexol (350 mg I/mL, GE Pharmaceutical, Shanghai of China), at 1.3 mL per kilogram of body weight was used (total volume: 60-110 mL) at a flow rate of 2.5-4.5 mL/s was injected *via* a peripheral vein, using a dual high-pressure syringe. The AP acquisition time was triggered at 9 s after the attenuation of diaphragmatic abdominal aorta reached 100 HU (SmartPrep; GE Healthcare). The VP followed with a 30 s interval. Raw data were reconstructed to 1.25-mm slice images, using decompose projection-based software. An additional 40% adaptive statistical iterative reconstruction algorithm was applied to suppress image noise and decrease the radiation dose required for spectral CT.

Image analysis

All CT images were transferred to a commercially available workstation (Advantage Windows 4.6; GE Medical Systems, Chicago, IL, United States) to generate iodine-based MD images (Figures 1 and 2). Two experienced radiologists (J.G. and P.L., with 25 and 5 years of experience with abdominal CT, respectively), who were blinded to the pathological results, analyzed the images. Three manually drawn regions of interests (ROIs) that encompassed the maximum lesion in the consecutive 1.25-mm layers of bi-phasic axial images were measured. Areas containing prominent artifacts, necrosis, and vessels were carefully avoided (mean square: 871 mm^2; range: 122-1308 mm^2). For the normal site, we chose a distance longer than 5 cm from the lesion edge that was thick enough to place the ROI. Three small circular ROIs with a diameter exceeding 2 mm were measured as ROI-normal. Images were compared to ensure the measurements were as consistent as possible in both phases. The ICs in the AP (IC-AP) and in the VP (IC-VP) were generated simultaneously (unit: 100 μg/mL). At the same time, a round ROI was placed on the abdominal aorta in the same layer as the target, to calculate the normalized IC (nIC = IC_{target}/IC_{aorta})[15], aiming to reduce the individual circulatory variability. All the ICs and nICs obtained from the same patient were averaged and disagreement on measurement was resolved by consensus.

Histopathologic evaluation

A surgeon (K.R) and a radiologist (X.C) performed sampling together to guarantee that the specimen and the ROI were from virtually the same level, by re-examining the axial and multi-planar reconstruction images. The distance to the cardia or pylorus of the sample site and the thickness were compared on both CT images and surgical specimens. Then, the selected samples (tumor and normal wall) were fixed overnight in 10% formalin, and subsequently dehydrated in alcohol and paraffin-embedded. Wax blocks comprising the central part of the adenocarcinoma were sectioned into 4-μm-thick slices. A ready-to-use two-step streptavidin-peroxidase method was applied. The mouse anti-CD34 monoclonal antibody (diluted 1:150) and rabbit anti-VEGF-A polyclonal antibody (diluted 1:200) (Beijing Zhongshan Goldenbridge Company, Beijing, China) were used to stain all pathological tissues. Positive and negative immunohistochemistry controls were prepared as routine. A pathologist (K.C, with 25 years' experience in MVD and VEGF immunostaining), who was blinded to the spectral CT imaging results, performed the counting and evaluation of all slides.

MVD counting was performed using the Weidner method[16]. The area where vascular endothelial cells stained most intensively was first identified at low (× 100) magnification. Then, five fields were randomly selected at × 400 magnification to count the CD34-positive cell clusters and the mean was recorded as the final value (Figures 1 and 2). VEGF (stained brown), located in the cytoplasm, was scored using an established method[17]: scores of the percentage of positive tumor cells and signal intensity were summed. If the score was less than 4, the section was considered negative, whereas a score of 4 or more was considered positive (Figures 1 and 2).

Statistical analysis

All statistical procedures were performed with a software package (SPSS 21.0, Chicago, IL, United States).

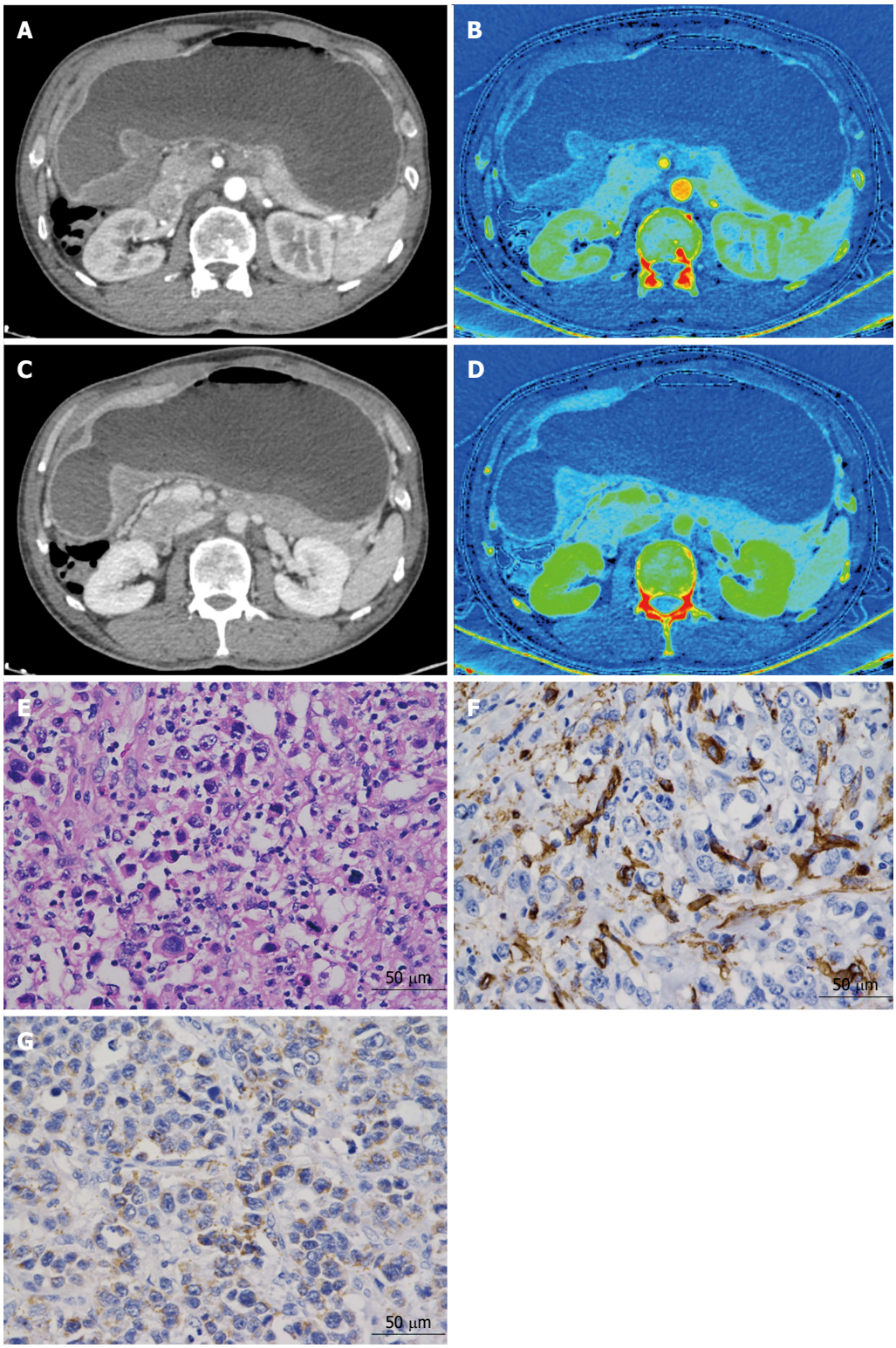

Figure 1 Detection of the iodine concentration value in a 51-year-old man with poorly differentiated adenocarcinoma, with staging Ⅲc (T4aN3M0). A: The monochromatic image shows focal wall thickening in the gastric antrum; B: The iodine-water image with iodine concentration (IC) value 12.83 (100 μg/cm^3), normalized IC (nIC) value 0.11 in the arterial phase. Monochromatic image (C) and iodine-water image (D) with IC value 23.91 (100 μg/cm^3), nIC value 0.53 in the venous phase; E: Hematoxylin and eosin staining of a pathological section obtained from radical surgery shows poorly differentiated, diffused subtype in the Lauren classification (× 400); F: CD34-staining shows endothelial cells stained brown; micro-vessels form clusters or have tiny hollow lumens (micro-vessel density 45/magnification × 400). G: Weak vascular endothelial growth factor staining in the cytoplasm (× 400) with score 2.

A *P*-value of less than 0.05 was considered to indicate a statistically significant difference. Nodal status was classified as positive and negative for lymph node metastasis, and the depth of invasion was classified as positive and negative serosal involvement. A single highly differentiated patient was grouped together

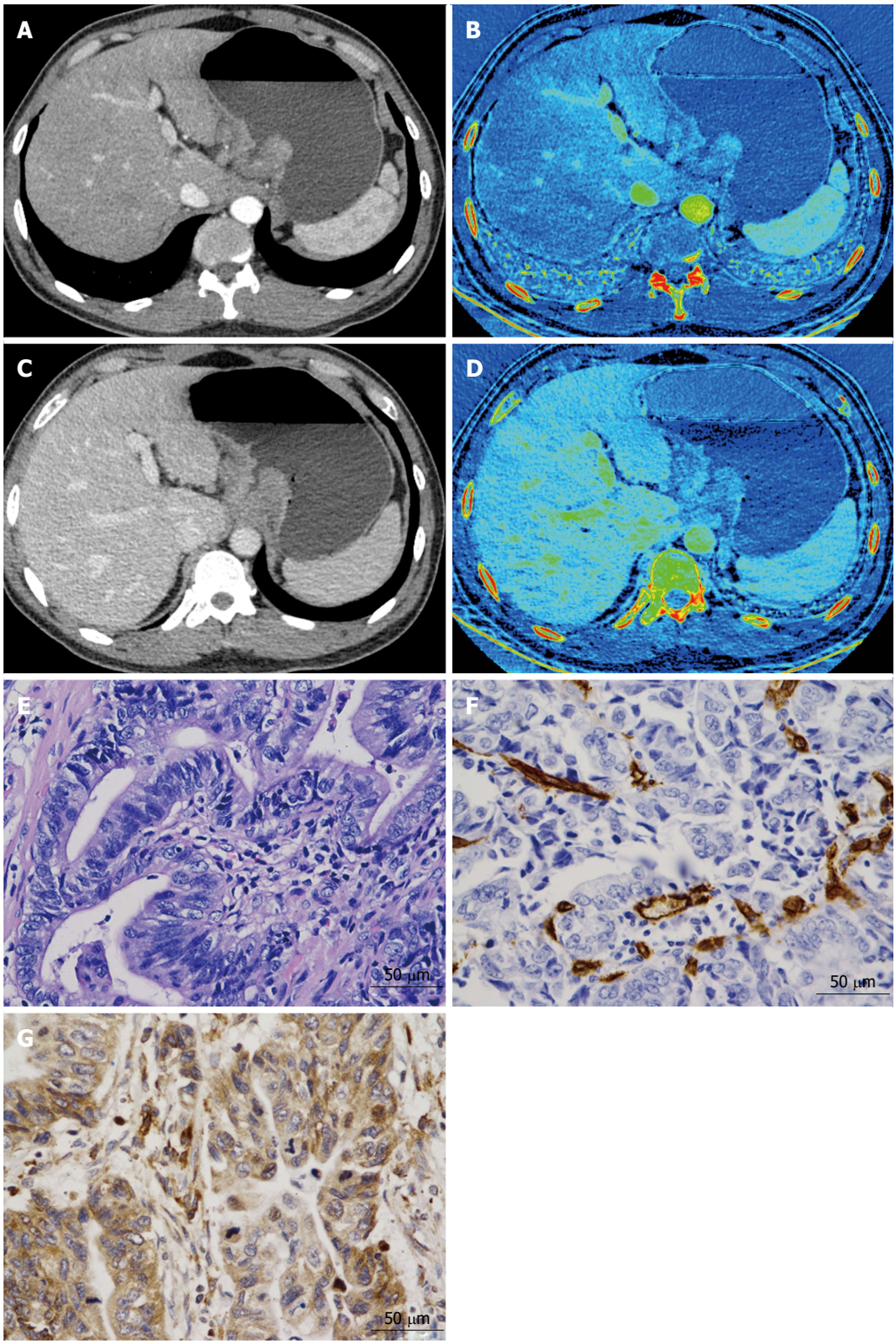

Figure 2 Detection of iodine concentration value in a 50-year-old man with moderate differentiated adenocarcinoma, of staging Ⅲa (T4aN1M0). A: Monochromatic image shows focal wall thickening in the gastric cardia and lesser curvature; B: The iodine-water image with iodine concentration (IC) value 11.78 (100 μg/cm^3), normalized IC (nIC) value 0.09 in the arterial phase; Monochromatic image (C) and (D) iodine-water image with IC value 18.63 (100 μg/cm^3), nIC value 0.34 in the venous phase; E: Hematoxylin and eosin staining shows a moderately differentiated, intestinal Lauren subtype (× 400); F: Immunohistochemical staining shows CD34 positive micro-vessel (micro-vessel density count: 27/magnification × 400); G: Strongly positive vascular endothelial growth factor staining (× 400) with score 5.

with the moderately differentiated patients. Data were subjected to a Kolmogorov-Smirnov normality test and continuous variables were presented as means and standard errors of the mean. When analyzing the correlation of nIC and MVD and VEGF, scatter plots were made first between continuous variables, followed by the Pearson or the Spearman rank-correlation test (Figure 3). Student's *t*-test, correct *t* test, and one-way

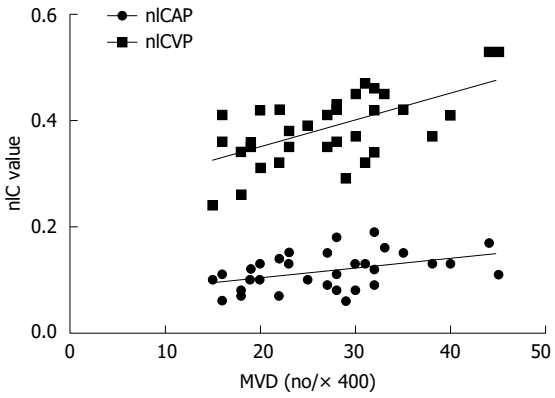

Figure 3 Scatter plots of normalized iodine concentration in arterial phase, normalized iodine concentration in venous phase, and microvessel density counts in tumor lesions (r = 0.423 for normalized iodine concentration in arterial phase, r = 0.606 for normalized iodine concentration in venous phase). VEGF: Vascular endothelial growth factor; nIC: Normalized iodine concentration; nIC-AP: nIC-arterial phase; nIC-VP: nIC-venous phase; MVD: Microvessel density.

analysis of variance (ANOVA)-LSD test were performed to analyze differences in categorical data between groups (serosal involvement, lymph node metastasis, histologic differentiation, Lauren subtype, tumor location, and gender).

RESULTS

A total of 34 advanced GC patients (23 males, 11 females; mean age: 56 ± 3.7 years; age range: 30-73 years) were included (Table 1). Tumor size ranged from 1.5 cm to 13.0 cm (median: 4.0 cm). Fourteen tumors located in the gastric cardia-fundus, nine in the gastricum, and 11 in antrum. All patients were treated surgically by radical gastrectomy and D2 lymph node dissection. Based on pathologic results, the adenocarcinoma was well differentiated in one patient, moderately differentiated in 16 patients, and poorly differentiated in 17 patients. According to the 7th American Joint Committee on staging classification (AJCC), five patients were classified as T2, two as T3, twenty-two as T4a and five as T4b; eleven as N0, eight as N1, seven as N2, and eight as N3. No patient had distant metastasis. The Lauren classification was as follows: 15 were intestinal type, seven were mixed type, and 12 were diffuse type. Additionally, the immunostaining analysis revealed that 25 patients (73.53%) stained positive for VEGF with a score of 4 (n = 11), 5 (n = 9), or 6 (n = 5). The mean MVD count for these 34 tumors was 26.94 ± 1.35.

In general, the bi-phasic nIC values and the MVD counts were positively correlated (P = 0.013, P < 0.001, respectively). VEGF did not correlate with either nIC value or with MVD, as shown in Table 2. When stratified by different clinical features, the correlation coefficient value increased. nIC-AP positively correlated with MVD in patients with tumor stage less than T4 (r = 0.851, P = 0.015), tumor of N0 stage (r = 0.620, P = 0.042), with a tumor located in the pylorus region (r = 0.616, P = 0.044), and who were female (r = 0.696, P = 0.017). On the other hand, nIC-VP correlated with MVD in the more advanced group of patients, with tumors above T4 stage (r = 0.656, P < 0.001), with nodular involvement (r = 0.644, P = 0.001), that were poorly differentiated (r = 0.799, P < 0.001), were of mixed and diffused Lauren subtypes (r = 0.827, P = 0.022; r = 0.765, P = 0.004, respectively), and male gender (r = 0.606, P = 0.002), as shown in Table 3.

The nIC values in the primary GC and normal gastric wall were 0.116 ± 0.033 and 0.101 ± 0.023 in arterial phase (P = 0.033), 0.386 ± 0.061, and 0.286 ± 0.066 in the venous phase (P < 0.001) (Figure 4A). For the VEGF-positive and -negative group, neither nIC-AP nor nIC-VP showed statistically significant differences (Figure 4B).

When stratified by clinical subgroups, both nIC-AP and nIC-VP were higher in patients with serosal involvement, lymph node metastasis, poor differentiation, and diffused Lauren type than in those with depth invasion under T4, nodal status N0, high and moderate differentiation, intestinal and mixed Lauren type, but these differences did not reach statistical significance.

Table 1 Clinical characteristics of the patients (n = 34)

Sex	Male	23	67.65%
	Female	11	32.35%
Age	30 -73 yr (56 ± 3.7 yr)		
Size	1.5 -13.0 cm (median 4.0 cm)		
Tumor location	Cardia/Fundus	14	41.18%
	Gastricum	9	26.47%
	Antrum	11	32.35%
Nodal status	N0	11	32.35%
	N1	8	23.53%
	N2	7	20.59%
	N3	8	23.53%
Depth of invasion	pT2	5	14.71%
	pT3	2	5.89%
	pT4a	22	64.71%
	pT4b	5	14.71%
Lauren subtype	Intestinal type	15	44.12%
	Mixed type	7	20.59%
	Diffuse type	12	35.29%
Histological grading	Highly differentiated	1	2.38%
	Moderately differentiated	16	47.06%
	Poorly differentiated	17	50.00%

Table 2 Correlation of nIC values, microvessel density and vascular endothelial growth factor expression

Varieties	MVD		VEGF	
	r	P value	r	P value
nIC-AP	0.423	0.013[a]	0.170	0.358
nIC-VP	0.606	0.000[a]	0.311	0.073
MVD	1.000		0.210	0.233

[a]P < 0.05. nIC-AP: Normalized iodine concentration in arterial phase; nIC-VP: Normalized iodine concentration in venous phase; MVD: Microvessel density; VEGF: Vascular endothelial growth factor.

Table 3 Correlations between bi-phase normalized iodine concentration and microvessel density in different clinical-pathological subgroups

Varieties	*n*	nIC-AP *vs* MVD		nIC-VP *vs* MVD	
		r	*P* value	*r*	*P* value
Depth of invasion					
< T4	7	0.851	0.015[a]	0.600	0.154
T4	27	0.370	0.057	0.656	0.000[a]
Nodal status					
N0	11	0.620	0.042[a]	0.600	0.051
N1-3	23	0.330	0.124	0.644	0.001[a]
Histologic differentiation					
Highly and Moderately differentiated	17	0.250	0.334	0.190	0.466
Poorly differentiated	17	0.427	0.087	0.799	0.000[a]
Lauren subtype					
Intestinal type	15	0.222	0.427	0.101	0.719
Mixed type	7	0.741	0.057[a]	0.827	0.022[a]
Diffuse type	12	0.145	0.653	0.765	0.004[a]
Tumor location					
Cardia/Fundus	14	0.311	0.279	0.760	0.796
Gastricum	9	0.385	0.307	0.507	0.163
Antrum	11	0.616	0.044[a]	0.891	0.000[a]
Sex					
Male	23	0.385	0.070	0.606	0.002[a]
Female	11	0.696	0.017[a]	0.605	0.049

[a]$P < 0.05$. nIC-AP: Normalized iodine concentration in arterial phase; nIC-VP: Normalized iodine concentration in venous phase; MVD: Microvessel density.

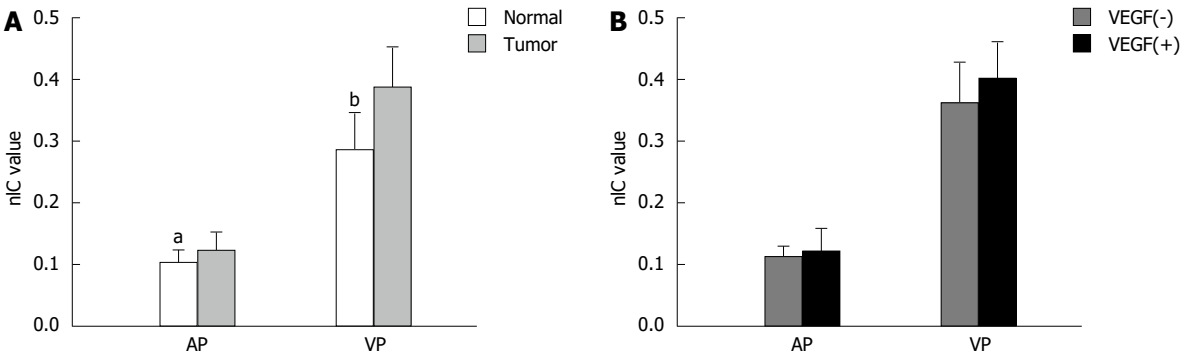

Figure 4 Comparison of normalized iodine concentration in arterial phase; and normalized iodine concentration in venous phase between the normal gastric wall and tumor site (A); comparison of normalized iodine concentration in arterial phase and normalized iodine concentration in venous phase between the vascular endothelial growth factor-positive and -negative group (B). [a]$P < 0.05$, [b]$P < 0.001$. VEGF: Vascular endothelial growth factor; nIC: Normalized iodine concentration; AP: Arterial phase; VP: Venous phase.

nIC-AP and nIC-VP showed statistically significant differences between differentiation categories ($P = 0.003$, $P = 0.001$, respectively) and between Lauren subtypes ($P = 0.016$, $P = 0.006$, respectively). The LSD test revealed that nIC-AP and nIC-VP were significantly different between intestinal and diffuse Lauren subtypes ($P = 0.005$, $P = 0.004$, respectively). nIC-VP was also significantly different between intestinal and mixed Lauren subtypes ($P = 0.013$), as shown in Table 4.

DISCUSSION

There were four major findings from this study. First, the bi-phasic nICs showed a significantly linear positive relationship with MVD in primary GC. The nIC-AP and nIC-VP correlated with MVD in different subgroups; the former correlated significantly with MVD in the relative earlier stage of advanced GC, while the latter correlated with MVD in the more advanced stage. Second, no significant correlation was found between nICs and VEGF. Third, nIC values in the normal gastric wall were observed to be significant lower than that in the tumor. Fourth, nICs were observed to differ between histological grades and Lauren subtypes of advanced GC; the greater the malignancy, the higher the nICs. Taken together, these observations demonstrate that quantification of iodine in spectral CT imaging have the potential to reflect angiogenesis of advanced GC.

Iodine, a commonly used CT contrast material, is generally known to produce higher attenuation at low tube voltage settings[18]. Based on this effect, spectral CT using high and low voltage switching settings could

Table 4 Difference of bi-phase normalized iodine concentration between different clinical-pathological subgroups

Varieties	*n*	nIC-AP		nIC-VP	
		mean ± SD	*P* value	mean ± SD	*P* value
Depth of invasion					
< T4	7	0.101 ± 0.042	0.195	0.363 ± 0.079	0.302
> T4	27	0.120 ± 0.031		0.392 ± 0.063	
Nodal status					
N0	11	0.112 ± 0.033	0.321	0.385 ± 0.085	0.923
N1-3	23	0.125 ± 0.035		0.387 ± 0.057	
Histologic differentiation					
Highly and moderately differentiated	17	0.100 ± 0.028	0.003[a]	0.352 ± 0.048	0.001[a]
Poorly differentiated	17	0.132 ± 0.031		0.421 ± 0.065	
Lauren subtype					
Intestinal type	15	0.099 ± 0.029	0.016[a]	0.347 ± 0.048	0.006[a]
Mixed type	7	0.120 ± 0.032		0.417 ± 0.061	0.013[1,a]
Diffuse type	12	0.135 ± 0.030	0.005[2,a]	0.417 ± 0.067	0.00[2,a]
Tumor location					
Cardia/Fundus	14	0.109 ± 0.033	0.445	0.385 ± 0.046	0.874
Gastricum	9	0.128 ± 0.024		0.387 ± 0.064	
Antrum	11	0.116 ± 0.040		0.387 ± 0.091	
Sex					
Male	23	0.113 ± 0.033	0.377	0.390 ± 0.069	0.633
Female	11	0.124 ± 0.035		0.378 ± 0.062	

[1]One-way ANOVA-LSD, mixed type *vs* intestinal type; [2]Diffuse type *vs* intestinal type. [a]$P < 0.05$. nIC-AP: Normalized iodine concentration in arterial phase; nIC-VP: Normalized iodine concentration in venous phase; MVD: Microvessel density; SD: Standard deviation.

differentiate materials of the same density[19] and the IC value could be extracted[20]. With water-iodine based material decomposition images, Lv *et al*[9] concluded that the IC in images of hepatic lesions acquired in a quantitative parameter was highly precise. Thieme *et al*[21] found a very good correlation between vessel occlusion depicted at CTA and IC defects in the dual-energy image, indicating that iodine distribution in the parenchyma is closely related to pulmonary perfusion. Therefore, the IC may be considered as an indirect marker of perfusion and tumor vascularity.

Tumor angiogenesis is defined as the formation of new blood vessels from pre-existing vessels[22]. MVD and identification of VEGF in tissues are commonly used biomarkers of angiogenesis[23]. In previous studies, the relationships between dynamic contrast-enhanced perfusion CT parameters and immunohistological markers of angiogenesis have been studied in different tumors, including colorectal cancer[24], advanced GC[6,25], lung cancer[26], *etc.* However, the studies produced discrepant results on whether the use of blood flow or permeability surface area product were efficacious.

Our results proved a positive linear relationship between IC and MVD in primary GC. The nIC values were significantly elevated in the tumor as compared to the normal gastric wall. Similar results were acquired by Pang *et al*[27], who considered the nIC value of the infarcted myocardium to be an important indicator of MVD in the 1-min and 3-min CT images. Additionally, the study by Hu *et al*[12] indicated that the nIC values of three-phase scans had a positive correlation with MVD for detecting the therapeutic response in a pancreatic carcinoma xenograft nude mouse model. Taken together, spectral CT imaging can be used to evaluate angiogenesis in disease.

On the other hand, nIC had a low correlation with VEGF expression, and no significant differences were found in the comparison between IC parameters and VEGF group. VEGF, one of the most prominent biomarkers of angiogenesis studied to date, has been shown to correlate well with CT perfusion in peripheral pulmonary nodules[28]. Moreover, the study of Zhou *et al*[13] in a rabbit VX2 liver model suggested that nIC and contrast-enhanced ultrasound parameters positively correlated with VEGF and FGF2 expression, while several reports failed to show such a correlation, for example, the GC study performed by Yao *et al*[6] and the colorectal cancer research by Goh *et al*[24]. The relationship between VEGF expression and imaging of tumor vascularity is complex. Further investigations of IC and VEGF in a large population with different clinical-pathology are needed.

At the same time, nIC in arterial phase and venous phase displayed different character when stratified. The nIC-AP showed correlations with MVD in relative earlier and differentiated advanced GC, while nIC-VP correlated with MVD in more advanced stage and poorly differentiated advanced GC.

In terms of the acquisition time of our routine abdominal CT scanning, the AP was performed at about 25-30 s after contrast media injection, when the mucosa at the lesion presented as a focal enhanced line. nIC-AP can reflect the blood supply and functional capillary density. In the VP of GC, the markedly increased interstitial fibrous tissue reduced the flow-out speed of the contrast media[29]; thus, more dysfunctional neo-vessels should be considered. Therefore, the nIC-VP may represent the distribution of iodine in

interstitial spaces. Under such conditions, the bi-phasic nIC demonstrated the vascular character of GC, and nIC-VP may be better correlated with MVD in advanced GC.

Furthermore, both nICs were different between histological differentiations and Lauren subgroups. The nIC-VP was more effective than nIC-AP in displaying the difference between Lauren subtypes. In general, the nIC value was higher in poorly differentiated and diffused types than that in highly or moderately differentiated and intestinal types. A previous study[30] has found that the degree of tumor angiogenesis was closely related to the pathological grade, that is, the poorer the differentiation of the tumor, the higher the MVD values. Another study[31] demonstrated a correlation between MVD and tumor histological type according to the Lauren classification. Accordingly, it is likely that the nIC value can be used to evaluate histology by mapping the neovascularization of advanced GC. The finding in the present study was also supported by the results of Pan *et al*[15] and Wang *et al*[32] in GC research.

The nICs increased in patients with serosal involvement and lymphatic metastasis, but the differences from patients without serosal involvement and lymphatic metastasis did not reach significant difference, for reasons that are not immediately clear, as these clinical-pathological features should reflect the functional status of the vasculature. Both nIC-AP and nIC-VP correlated with MVD of GC located in the antrum and occurring in different genders. However, nICs were not very effective in differentiating between these groups.

There are several potential limitations in our study. First, the tumor vasculature is spatially heterogeneous. Although we selected specimens carefully under the guide of two major specialists, the excision level was barely achieved. It may be questioned whether the part of the histopathological part selected and matched to the imaging measurement represented the angiogenesis of the whole tumor. Second, the sample numbers were limited, especially when subdivided by clinical classification. A larger prospective investigation is needed to confirm the present findings. Third, given the limitations of CT resolution, flat and light ulcerous lesions without enhancement would have been missed in the images, which inducing selection bias.

In conclusion, the bi-phasic nIC values had a positive linear correlation with MVD. nIC-AP reflected the angiogenesis in relatively earlier and well-differentiated advanced GC, while nIC-VP reflected this in further advanced and poorly differentiated GC. Spectral CT with quantitative IC value offers a new choice to evaluate the angiogenesis of gastric cancer noninvasively.

COMMENTS

Background

Angiogenesis is fundamental to the growth, invasion, and metastasis of gastric cancer (GC). To date, the standard method for studying angiogenesis has been histopathological counting of micro-vessel density (MVD). This is impractical for patients who undergoing anti-angiogenesis or chemotherapy. The current trial was designed to evaluate if the iodine concentration (IC) generated by spectral computed tomography could non-invasively judge the features of tumoral MVD and vascular endothelial growth factor with clinical data.

Research frontiers

Iodine-water material-decomposition (MD) images can quantitatively map the IC of the tissue in enhanced scanning. In this study, there is suggestion that IC value has the potential to reflect angiogenesis of advanced GC.

Innovations and breakthroughs

The authors measured the normalized IC value in spectral computed tomography (CT) with manually drawn regions of interests to avoid the selection bias. Data stratified by clinical subgroups further revealed the connection between imaging index and patho-index. They finally proved that the normalized IC value in different scanning phase could reflect angiogenesis in different pathological subgroups of advanced GC.

Applications

Radiological-pathological correlation in angiogenesis, although with not much high coefficient, will offer a new choice to clinical decision in judging the status of GC, especially for neoadjuvant chemotherapy or radiochemotherapy patients.

Terminology

IC: Iodine is a commonly used contrast material in performing enhanced CT scanning. The iodine concentration here refers an imaging data, representing iodine distribution of the organ with spectral CT modality, not the real iodine concentration of contrast material itself.

Peer-review

The study on the spectral computed tomography in advanced gastric cancer is quite interesting with novelties.

REFERENCES

1 **Torre LA**, Bray F, Siegel RL, Ferlay J, Lortet-Tieulent J, Jemal A. Global cancer statistics, 2012. *CA Cancer J Clin* 2015; **65**: 87-108 [PMID: 25651787 DOI: 10.3322/caac.21262]

2 **Chen W**, Zheng R, Zeng H, Zhang S. The updated incidences and mortalities of major cancers in China, 2011. *Chin J Cancer* 2015; **34**: 502-507 [PMID: 26370301 DOI: 10.1186/s40880-015-0042-6]

3 **Carmeliet P**, Jain RK. Molecular mechanisms and clinical applications of angiogenesis. *Nature* 2011; **473**: 298-307 [PMID: 21593862 DOI: 10.1038/nature10144]

4 **Hattori Y**, Gabata T, Matsui O, Mochizuki K, Kitagawa H, Kayahara M, Ohta T, Nakanuma Y. Enhancement patterns of pancreatic adenocarcinoma on conventional dynamic multidetector row CT: correlation with angiogenesis and fibrosis. *World J Gastroenterol* 2009; **15**: 3114-3121 [PMID: 19575490 DOI: 10.3748/wjg.v15.i25.3114]

5 **Kim JW**, Jeong YY, Chang NK, Heo SH, Shin SS, Lee JH, Hur YH, Kang HK. Perfusion CT in colorectal cancer: comparison of perfusion parameters with tumor grade and microvessel density. *Korean J Radiol* 2012; **13** Suppl 1: S89-S97 [PMID: 22563293 DOI: 10.3348/kjr.2012.13.S1.S89]

6 **Yao J**, Yang ZG, Chen HJ, Chen TW, Huang J. Gastric adenocarcinoma: can perfusion CT help to noninvasively evaluate tumor angiogenesis? *Abdom Imaging* 2011; **36**: 15-21 [PMID: 20336293 DOI: 10.1007/s00261-010-9609-5]

7 **Lv P**, Lin X, Gao J, Chen K. Spectral CT: preliminary studies in the liver cirrhosis. *Korean J Radiol* 2012; **13**: 434-442 [PMID: 22778565 DOI: 10.3348/kjr.2012.13.4.434]

8 **Zhang XF**, Lu Q, Wu LM, Zou AH, Hua XL, Xu JR. Quantitative iodine-based material decomposition images with spectral CT imaging for differentiating prostatic carcinoma from benign

prostatic hyperplasia. *Acad Radiol* 2013; **20**: 947-956 [PMID: 23830601 DOI: 10.1016/j.acra.2013.02.011]
9 **Lv P**, Lin XZ, Li J, Li W, Chen K. Differentiation of small hepatic hemangioma from small hepatocellular carcinoma: recently introduced spectral CT method. *Radiology* 2011; **259**: 720-729 [PMID: 21357524 DOI: 10.1148/radiol.11101425]
10 **Cai XR**, Feng YZ, Qiu L, Xian ZH, Yang WC, Mo XK, Wang XB. Iodine Distribution Map in Dual-Energy Computed Tomography Pulmonary Artery Imaging with Rapid kVp Switching for the Diagnostic Analysis and Quantitative Evaluation of Acute Pulmonary Embolism. *Acad Radiol* 2015; **22**: 743-751 [PMID: 25772582 DOI: 10.1016/j.acra.2015.01.012]
11 **Tang L**, Li ZY, Li ZW, Zhang XP, Li YL, Li XT, Wang ZL, Ji JF, Sun YS. Evaluating the response of gastric carcinomas to neoadjuvant chemotherapy using iodine concentration on spectral CT: a comparison with pathological regression. *Clin Radiol* 2015; **70**: 1198-1204 [PMID: 26188843 DOI: 10.1016/j.crad.2015.06.083]
12 **Hu S**, Huang W, Chen Y, Song Q, Lin X, Wang Z, Chen K. Spectral CT evaluation of interstitial brachytherapy in pancreatic carcinoma xenografts: preliminary animal experience. *Eur Radiol* 2014; **24**: 2167-2173 [PMID: 24903229 DOI: 10.1007/s00330-014-3257-z]
13 **Zhou Y**, Gao JB, Xu H, Dong JQ, Wang MY. Evaluation of neovascularization with spectral computed tomography in a rabbit VX2 liver model: a comparison with real-time contrast-enhanced ultrasound and molecular biological findings. *Br J Radiol* 2015; **88**: 20140548 [PMID: 26456032 DOI: 10.1259/bjr.20140548]
14 **Li GJ**, Gao J, Wang GL, Zhang CQ, Shi H, Deng K. Correlation between vascular endothelial growth factor and quantitative dual-energy spectral CT in non-small-cell lung cancer. *Clin Radiol* 2016; **71**: 363-368 [PMID: 26873627 DOI: 10.1016/j.crad.2015.12.013]
15 **Pan Z**, Pang L, Ding B, Yan C, Zhang H, Du L, Wang B, Song Q, Chen K, Yan F. Gastric cancer staging with dual energy spectral CT imaging. *PLoS One* 2013; **8**: e53651 [PMID: 23424614 DOI: 10.1371/journal.pone.0053651]
16 **Weidner N**, Semple JP, Welch WR, Folkman J. Tumor angiogenesis and metastasis--correlation in invasive breast carcinoma. *N Engl J Med* 1991; **324**: 1-8 [PMID: 1701519 DOI: 10.1056/NEJM199101033240101]
17 **Suzuki S**, Dobashi Y, Hatakeyama Y, Tajiri R, Fujimura T, Heldin CH, Ooi A. Clinicopathological significance of platelet-derived growth factor (PDGF)-B and vascular endothelial growth factor-A expression, PDGF receptor-β phosphorylation, and microvessel density in gastric cancer. *BMC Cancer* 2010; **10**: 659 [PMID: 21118571 DOI: 10.1186/1471-2407-10-659]
18 **Nakayama Y**, Awai K, Funama Y, Hatemura M, Imuta M, Nakaura T, Ryu D, Morishita S, Sultana S, Sato N, Yamashita Y. Abdominal CT with low tube voltage: preliminary observations about radiation dose, contrast enhancement, image quality, and noise. *Radiology* 2005; **237**: 945-951 [PMID: 16237140 DOI: 10.1148/radiol.2373041655]
19 **Zhang Y**, Cheng J, Hua X, Yu M, Xu C, Zhang F, Xu J, Wu H. Can Spectral CT Imaging Improve the Differentiation between Malignant and Benign Solitary Pulmonary Nodules? *PLoS One* 2016; **11**: e0147537 [PMID: 26840459 DOI: 10.1371/journal.pone.0147537]
20 **Agrawal MD**, Pinho DF, Kulkarni NM, Hahn PF, Guimaraes AR, Sahani DV. Oncologic applications of dual-energy CT in the abdomen. *Radiographics* 2014; **34**: 589-612 [PMID: 24819783 DOI: 10.1148/rg.343135041]
21 **Thieme SF**, Johnson TR, Lee C, McWilliams J, Becker CR, Reiser MF, Nikolaou K. Dual-energy CT for the assessment of contrast material distribution in the pulmonary parenchyma. *AJR Am J Roentgenol* 2009; **193**: 144-149 [PMID: 19542406 DOI: 10.2214/AJR.08.1653]
22 **Lee TY**, Purdie TG, Stewart E. CT imaging of angiogenesis. *Q J Nucl Med* 2003; **47**: 171-187 [PMID: 12897709]
23 **Blank S**, Deck C, Dreikhausen L, Weichert W, Giese N, Falk C, Schmidt T, Ott K. Angiogenic and growth factors in gastric cancer. *J Surg Res* 2015; **194**: 420-429 [PMID: 25577146 DOI: 10.1016/j.jss.2014.11.028]
24 **Goh V**, Halligan S, Daley F, Wellsted DM, Guenther T, Bartram CI. Colorectal tumor vascularity: quantitative assessment with multidetector CT--do tumor perfusion measurements reflect angiogenesis? *Radiology* 2008; **249**: 510-517 [PMID: 18812560 DOI: 10.1148/radiol.2492071365]
25 **Zhang H**, Pan Z, Du L, Yan C, Ding B, Song Q, Ling H, Chen K. Advanced gastric cancer and perfusion imaging using a multidetector row computed tomography: correlation with prognostic determinants. *Korean J Radiol* 2008; **9**: 119-127 [PMID: 18385558 DOI: 10.3348/kjr.2008.9.2.119]
26 **Li Y**, Yang ZG, Chen TW, Chen HJ, Sun JY, Lu YR. Peripheral lung carcinoma: correlation of angiogenesis and first-pass perfusion parameters of 64-detector row CT. *Lung Cancer* 2008; **61**: 44-53 [PMID: 18055062 DOI: 10.1016/j.lungcan.2007.10.021]
27 **Pang LF**, Zhang H, Lu W, Yang WJ, Xiao H, Xu WQ, Chen Y, Liu Y, Bu YL, Pan ZL, Chen KM, Yan FH. Spectral CT imaging of myocardial infarction: preliminary animal experience. *Eur Radiol* 2013; **23**: 133-138 [PMID: 22814826 DOI: 10.1007/s00330-012-2560-9]
28 **Ma SH**, Le HB, Jia BH, Wang ZX, Xiao ZW, Cheng XL, Mei W, Wu M, Hu ZG, Li YG. Peripheral pulmonary nodules: relationship between multi-slice spiral CT perfusion imaging and tumor angiogenesis and VEGF expression. *BMC Cancer* 2008; **8**: 186 [PMID: 18590539 DOI: 10.1186/1471-2407-8-186]
29 **Monzawa S**, Omata K, Nakazima H, Yokosuka N, Ito A, Araki T. Advanced gastric cancer: the findings of delayed phase dynamic CT and radiologic-histopathologic correlation. *Nihon Igaku Hoshasen Gakkai Zasshi* 2000; **60**: 508-513 [PMID: 11019578]
30 **Du JR**, Jiang Y, Zhang YM, Fu H. Vascular endothelial growth factor and microvascular density in esophageal and gastric carcinomas. *World J Gastroenterol* 2003; **9**: 1604-1606 [PMID: 12854174 DOI: 10.3748/wjg.v9.i7.1604]
31 **Tenderenda M**, Rutkowski P, Jesionek-Kupnicka D, Kubiak R. Expression of CD34 in gastric cancer and its correlation with histology, stage, proliferation activity, p53 expression and apoptotic index. *Pathol Oncol Res* 2001; **7**: 129-134 [PMID: 11458276 DOI: 10.1007/BF03032579]
32 **Wang F**, Gao J, Liang P. Application value of CT spectrum curve and iodine measurement in the early diagnosis of gastric cancer. *Zhonghua Weichang Waike Zazhi* 2015; **18**: 243-247 [PMID: 25809327]

P- Reviewer: Kim SM **S- Editor**: Qi Y
L- Editor: A **E- Editor**: Liu WX

Published by **Baishideng Publishing Group Inc**
8226 Regency Drive, Pleasanton, CA 94588, USA
Telephone: +1-925-223-8242
Fax: +1-925-223-8243
E-mail: bpgoffice@wjgnet.com
Help Desk: http://www.wjgnet.com/esps/helpdesk.aspx
http://www.wjgnet.com

ISSN 1007-9327
09>